Journal of Alloys and Compounds 480 (2009) 922–927

Contents lists available at ScienceDirect

Journal of Alloys and Compounds

journal homepage: www.elsevier.com/locate/jallcom

Dynamic globularization kinetics during hot working of a two phase titanium alloy with a colony alpha microstructure

Hong-Wu Song, Shi-Hong Zhang*, Ming Cheng

Institute of Metal Research, Chinese Academy of Sciences, Shenyang, Liaoning 110016, PR China

ARTICLE INFO

Article history:
Received 14 January 2009
Received in revised form 15 February 2009
Accepted 18 February 2009
Available online 4 March 2009

Keywords:
High-temperature alloys
Microstructure
Kinetics
Strain

ABSTRACT

The dynamic globularization kinetics of Ti–6.5Al–1.5Zr–3.5Mo–0.3Si alloy with a colony alpha microstructure during deformation at temperature range of 920–980 °C and strain rate range of 0.01–10 s^{-1} was quantitatively characterized and investigated. The results show that both the globularization fraction and globularized grain size were sensitive to deformation conditions. At temperature higher than 950 °C, strain rates higher than 0.1 s^{-1} and true strain around 3, enhanced grain refinement was achieved through dynamic globularization. The refined structure shows improved superplasticity characteristics including near fully equaxied alpha grains around 1 μm, discontinues beta phase and high dislocation density at the globularized grain boundaries. The dynamic globularization kinetics characteristic was associated with deformation mechanism that controls the dynamic globularization process.

1. Introduction

Titanium alloys, particularly two phase titanium alloys have been widely used as advanced structural materials in aeronautic applications. Especially, the alloy with a nominal composition of Ti–6.5Al–1.5Zr–3.5Mo–0.3Si (named TC11 alloy), developed on the basis of the Russia alloy VT9, is a typical two phase alloy and has now been the most widely used titanium alloy in aerospace field in China to produce the compressor discs and blades. Due to the additions of beta isomorphous element Mo, neutral element Zr and beta eutectoid elements Si into Ti–6Al base, TC11 alloy has a higher strength, better creep resistance and more excellent thermal stability, especially at elevated temperatures compared with conventional Ti–6Al–4V alloy [1,2]

The lamellar microstructure associated with as-cast or beta-processed two phase titanium alloys has been found to break up or globularize both dynamically during deformation and statically during post deformation annealing in the alpha/beta phase field, which plays a key role in development of desired microstructure for final forming or service. Therefore, the globularization process has received considerable attention [3–7].

Many studies have investigated dynamic globularization of two phase titanium alloys. In early works, Kaybyshev et al. [8–10] studied the evolution of platelike microstructure during superplastic deformation (at strain rates in order of 10^{-3} s^{-1}) in the alpha/beta range of VT9 alloy at a qualitative level. The dynamic globularization process was found to be governed by the alpha → beta transformation and the development of grain boundary sliding. Semiatin et al. [11,12] observed that the dynamic globularization of Ti–6Al–4V alloy with colony alpha structure occurred at strain rate lower than 0.01 s^{-1}; strains around of the order of 0.75–1.0 and 2–2.5 were required respectively for 'initiation' and competition of dynamic globularization. Later study [13–15] indicated that the dependence of dynamic globularization kinetics on test temperature and initial microstructure appeared to be complex. Recently submicron grain structure was achieved by warm deformation of Ti–6Al–4V alloy at low temperature (550 °C) and low strain rate (0.001 s^{-1}) as a result of dynamic globularization [16]. It can be found that the former researches were focused on globularization behavior at low strain rate or warm temperature. However, most thermomechanical processing of two phase titanium alloys for ingot breakdown on hammer or hydraulic press in industry was carried out under high temperature and high strain rate (above 0.01 s^{-1}) conditions. Although the most recently research by Park et al. [17] showed enhanced superplasticity by dynamic globularization at high strain rate (0.1 s^{-1}) for Ti–6Al–4V alloy with martensite microstructure, quantitative analysis of dynamic globularization kinetics was still unclear under such conditions for alloys with colony alpha structure.

The object of present work is to quantitatively investigate dynamic globularization kinetics at strain rates higher than 0.01 s^{-1} of TC11 alloy with a colony alpha structure. In addition, the optimum processing parameters are determined within experimental conditions corresponding to significantly grain refinement by dynamic globularization.

* Corresponding author. Tel.: +86 24 83978266 fax: +86 24 23906831.
E-mail address: shzhang@imr.ac.cn (S.-H. Zhang).

0925-8388/$ – see front matter © 2009 Elsevier B.V. All rights reserved.
doi:10.1016/j.jallcom.2009.02.059

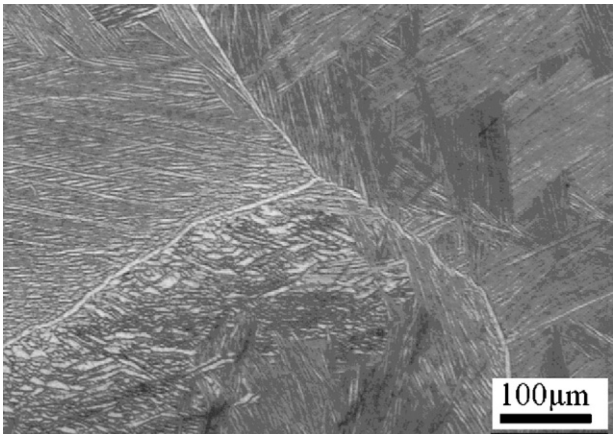

Fig. 1. Colony alpha structure of the heat treated wrought bars.

2. Experimental procedures

The chemical compositions (wt.%) of TC11 alloy used in this investigation are as follows: 6.17 Al, 3.41 Mo, 1.77 Zr, 0.285 Si, 0.054 Fe, 0.014 C, 0.01 N, 0.0006 H, 0.100 O, and balance Ti. The β transus temperature was measured about 1020 °C. The received wrought bars with a diameter of 10 mm were heated to 1040 °C, held for 30 min followed by furnace cooling. The initial microstructure of the heat treated material is given in Fig. 1. The microstructure shows a colony alpha structure consisting of lamellar alpha colonies in prior coarse β grains (average grain size about 500 μm), a grain boundary alpha layer (in thickness of 5 μm) and continuous beta layers in between the colony alpha lamellae (in thickness of 3 μm), which has a typical microstructure characteristic before cogging process in alpha/beta phase field.

Compression specimens machined from the heat treated bars were subjected to 30–80% isothermal hot compression tests on a Gleeble 3500 thermal simulator in the temperature range 920–980 °C and strain rate range 0.01–10 s^{-1}. The specimens were heated to test temperatures at a heating speed of 5 °C/s, held for 3 min, compressed to the given reduction and then water quenched to room temperature.

The deformed specimens were sectioned parallel to the compression axis for microstructural analysis. The samples for optical metallographic examination were made by mechanically polished and etched with a solution consisting of 10 pct HF, 20 pct HNO_3 and 60 pct H_2O. Because of the inhomogeneous deformation and non-uniform strain distribution in the compressed specimens, FEM was applied to calculate the local strains for microstructure observation. Since the beta phase transforms during cooling, it was mainly the primary alpha phase, which governs the structure type of the alloy, was studied. Globularization behavior of the alpha lamellae was then quantified using moderate magnification optical photographs by a quantitative metallographic image analysis system considering alpha phase with the aspect (length/width) ratio lower than 2 as a globular.

3. Results and discussion

3.1. Characterization of dynamic globularization kinetics

Micrographs at test temperatures of 920 °C and 980 °C at a large strain in Fig. 2 showed: partially globularization with fine globularized grains at low temperature (920 °C) and high strain rate (0.1 s^{-1}); near fully globularization with fine globularized grains at high temperature (980 °C) and high strain rate (0.1 s^{-1}); fully globularized structure with coarser alpha grains at low strain rates (0.01 s^{-1}) at both temperatures.

Quantitative measurements of the fraction globularized as a function of strain and globularized grain size at different strain rates and temperatures are summarized in Figs. 3 and 4. It revealed that a critical strain is needed for globularization initiation and both globularization fraction and globularized alpha grain size are very sensitive to deformation conditions.

It can be found in Fig. 3 that the globularization fraction increases with strain in a sigmoid way and it assumes that the globularized fraction f_g follows an Avrami type equation:

$$f_g = 1 - \exp[-k \cdot (\varepsilon - \varepsilon_c)^n] \quad (1)$$

Non-linear curve fitting using Eq. (1) shows a good agreement with the experimental results seen in Fig. 3. Thus, the critical strain

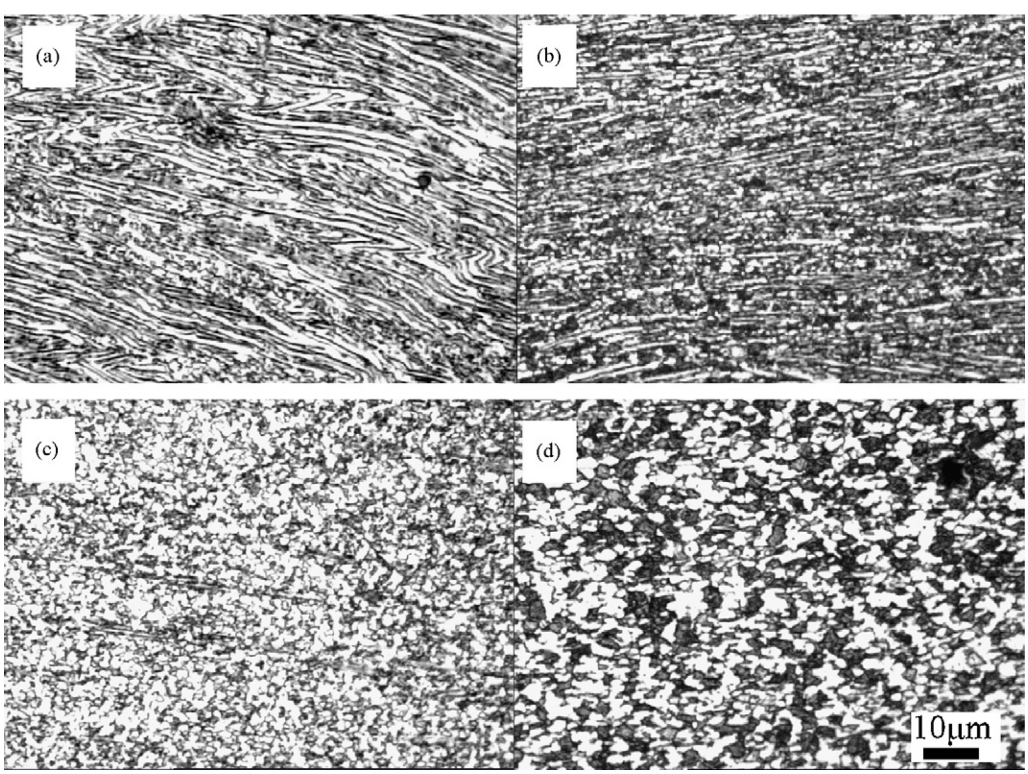

Fig. 2. Optical micrographs of structure developed in specimens compressed at temperatures of (a and c) 920 °C or (b and d) 980 °C and strain rates of (a and b) 0.1 s^{-1} or (c and d) 0.01 s^{-1}.

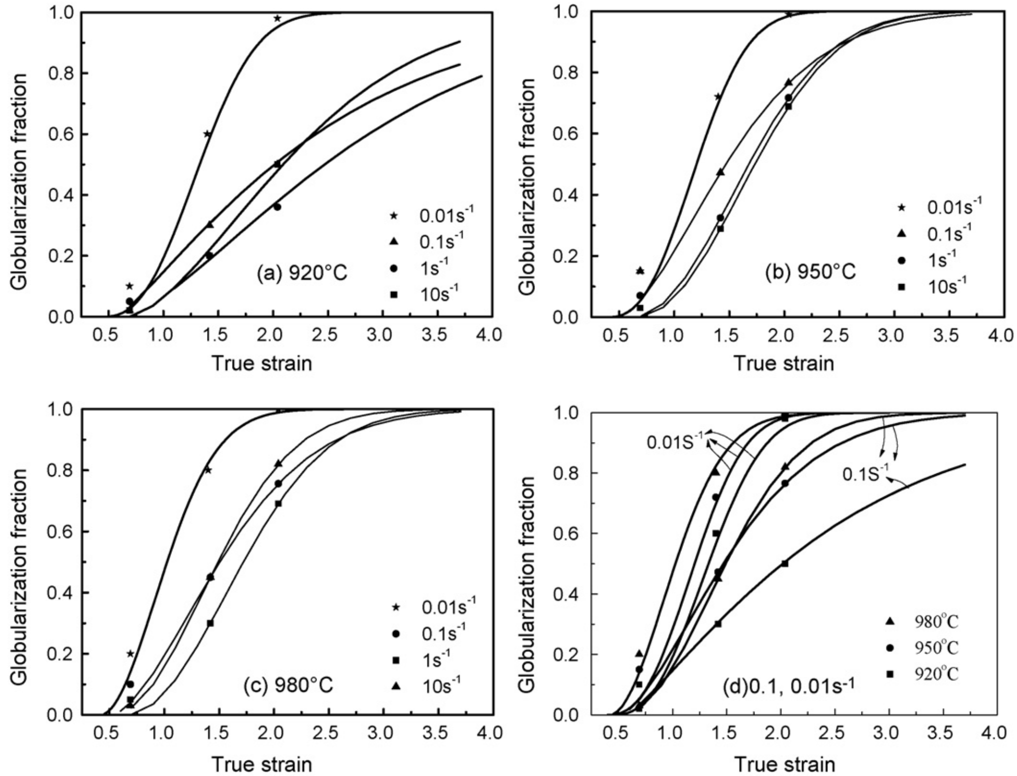

Fig. 3. Globularization fraction versus strain at different deformation conditions (dot—experimentally measured data, line—fitted result using Eq. (1)).

(to be ε_c in Eq. (1)) for initiation of globularization and the strain needed fully globularization (ε_f) was then predicted respectively using Eq. (1). The result is shown in Table 1.

3.2. Analysis of the critical strain

It reveals that a critical strain for initiation of globularization between 0.42–0.65 for all deformation conditions is needed (in Fig. 3) and the value shows relatively weak dependence on deformation temperature and strain rate (seen from Table 1). The same phenomenon was also found in [13] for Ti–6Al–4V alloy, although the critical strain reported is a little higher (~1.0) because of difference in alloys and the initial structures. In addition, the critical strain is much higher than peak strain (generally lower than 0.1) on the flow stress curves [13]. This phenomenon has big difference from general dynamic recrystallization (DRX) process, for which the critical strain is lower (less than the peak strain) and strongly dependent on deformation conditions. Thus, dynamic globularization may have different mechanism with DRX. During DRX process, critical strain is corresponding to critical dislocation density needed for new grain nucleation. Thus the critical strain value has strong dependence on deformation temperature and strain rate which affects the dynamic recovery behavior and dislocation density. While, for dynamic globularization involving a reduction in the aspect ratio of the plates, as suggested in [18], it can be interpreted in terms of geometric recrystallization, during which intraphase boundary forms as the first step instead of nucleation of new grains. The process is controlled by dislocation glide and therefore the limited sensitivity of critical strain to deformation temperature and strain rate may be rationalized on the basis that cumulative effect of the dislocation glide processes is related to strain magnitude per

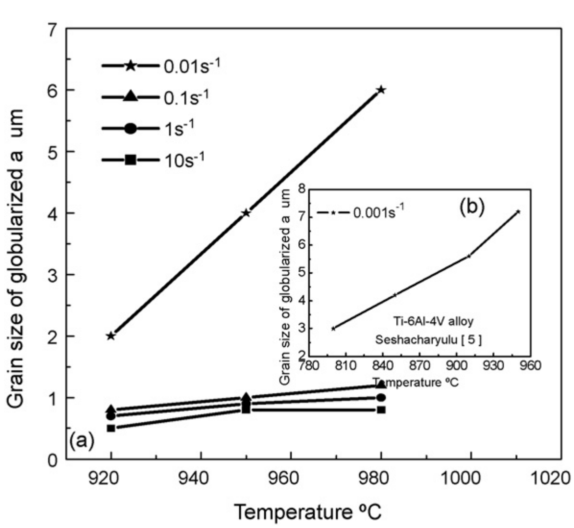

Fig. 4. Globularized grain size at different deformation conditions (a) measured in this study and (b) presented in the literature.

Table 1
Determined kinetic strain values using Eq. (1).

T, °C	$\dot{\varepsilon}$, s^{-1}	ε_c	ε_f
920	0.01	0.5	2.45
	0.1	0.6	4.25
	1	0.63	6.66
	10	0.65	4.23
950	0.01	0.45	2.23
	0.1	0.5	2.93
	1	0.55	3.07
	10	0.58	3.05
980	0.01	0.42	2.10
	0.1	0.5	2.67
	1	0.52	2.76
	10	0.55	2.88

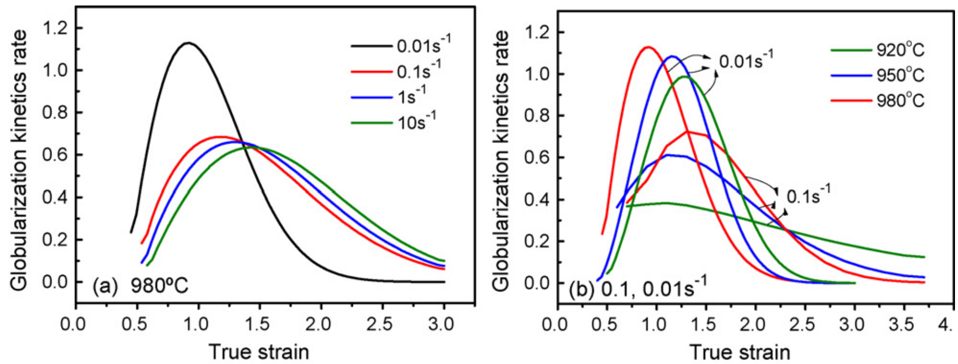

Fig. 5. Calculated kinetics rate as a function of strain at (a) 980 °C and (b) 0.1 and 0.01 s^{-1}.

se. It is also found that a large fraction of the lamellae has rotated to orientations perpendicular to the compression axis [18] at the critical strain levels needed for onset of dynamic globularization. It suggests that the reorientation of lamellae (in the form of lamellae kinking) also accounts for larger critical strain levels needed before globularization initiation.

3.3. Effect of deformation conditions on the globularized fraction

Seen from Fig. 3 and Table 1, the evolution of globularized fraction versus strain shows significantly dependence on deformation conditions. The globularization kinetics rate versus strain can be defined as:

$$v = \frac{\partial f_g}{\partial \varepsilon} \quad (2)$$

The calculated kinetics rate versus strain curves is shown in Fig. 5. The kinetics rate increases with decreasing strain rate, especially when the strain rate decreasing from 0.1 to 0.01 s^{-1} (also seen in Fig. 2). While, the dependence of kinetics on strain rate is not significant when strain rate is higher than 0.1 s^{-1} (in Figs. 5a and 3). The dependent of kinetics on temperature (in Figs. 5b and 3) is weak at strain rate 0.01 s^{-1} and at higher temperatures at 0.1 s^{-1} but with sharp decreasing when temperature drops from 950 to 920 °C. The kinetics rate then determines the dependence trend of ε_f on deformation conditions (shown in Table 1). The sensitivity of globularization kinetics on strain rate and temperature with sharp change, which is in contrast with the result in [8], could suggest that the dynamic recovery may play a significant role in globularization process which controls formation of intraphase boundary as a first step for globularization in the mechanism proposed by Weiss et al. [18].

It is also noted that the kinetics rate first increases and then decreases with strain increasing and has a peek value at a strain corresponding to 40–60% globularization. The same phenomenon has been reported in DRX process and was interpreted by a result of competition between the new grain nucleation rate and grain growth rate. As discussed above, there is no new grain nucleation during dynamic globularization. So, the decrease of kinetics speed after the peak value may be caused by reduction of aspect ratio of lamellae after certain amount of globularization which makes the continue fragmentation of lamellae more difficult. Another important reason may be that much part of deformation is exerted on globularized phase because of easier deformation ability of equiaxed grains than lamellae. Deformation mechanism analysis by Kim [19] also found that the grain boundary sliding of globularized grains took place after heavy deformation of Ti–6Al–4V alloy with colony alpha structures.

3.4. Effect deformation conditions on globularized grain size

The measured grain size of globularized alpha phase at different deformation conditions is shown in Fig. 4. It can be seen that the sharp change occurs in globularized grain size when the strain rate decreases from 0.1 s^{-1}. The globularized grain size in the strain rate range of 0.1–10 s^{-1} has a slight increase with temperature and remains around 1 μm. However, when the strain rate decreases to 0.01 s^{-1}, there is a sharp increase of globularized grain size with temperature up to 6 μm. When strain rate decreases further, even coarser globularized grain was found for Ti–6Al–4V alloy [5]. As

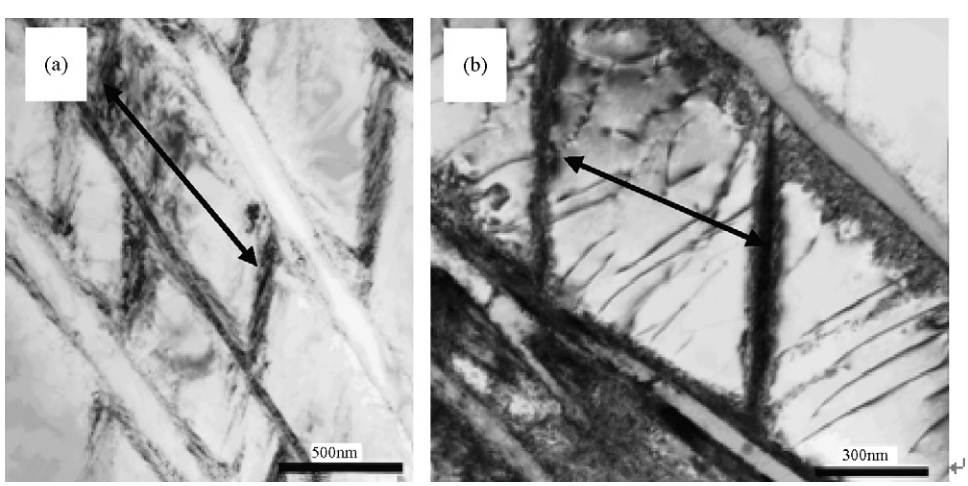

Fig. 6. TEM observations of alpha plate deformed at strain rate of (a) 0.01 s^{-1} or (b) 0.1 s^{-1} at strain of 0.69.

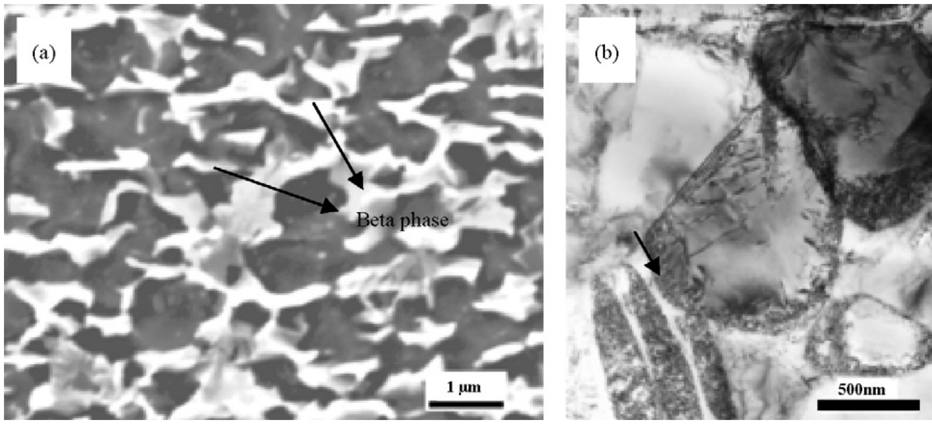

Fig. 7. Microstructure observations of the globularized structure in specimen deformed at 980 °C and 0.1 s^{-1} with a strain of 2.9 (a) SEM image and (b) TEM image.

proposed in [18], during globularization process, grooves formed on the surface of the alpha plates either by surface tension related effects or shear localization within the plates may serve to fragment the plates into nearly equiaxed regions via penetration of beta phase, with the diameter approximately equal to the plate thickness. However, as seen in Fig. 6, very close plate thickness (both around 0.4 μm) is found before globularization deformed at the same temperature and at strain rate 0.1 and 0.01 s^{-1}, respectively but with sharp difference in globularized grain size. So the fragment of alpha plates may indeed occur as suggested in [18], the globualrized grain size may not essentially equal to the plate thickness, and it is dependent on the aspect ratio of the fragment which finally becomes globular driven by surface energy. It can be seen from Fig. 6b, at strain rate 0.1 s^{-1}, the length of fragment is similar to plate thickness and the finally globularized grain size is more or less close to plate thickness. However, when deformed at 0.01 s^{-1}(Fig. 6a), the length of fragment is larger than plate thickness, thus a globularized grain size bigger than plate thickness could be readily anticipated. This difference in aspect ratio of plate fragment is caused by different dynamic recovery rate at two different strain rates. At higher strain rate, more dislocations are produced and the dislocation walls are denser due to poorer recovery rate and dislocations can still be found in short fragment formed by two adjacent dislocation walls in Fig. 6b. While at low strain rate, due to fast recovery rate, dislocation gliding and annihilation are easier, less amount of dislocation walls are formed, and nearly no dislocations can be found in the relatively longer plate fragment in Fig. 6a. When the deformation continues, the dislocation walls transfer to intraphaser boundaries and form lamellar fragment with different aspect ratios and finally different globular sizes.

3.5. Enhanced grain refinement through dynamic globularization

From kinetics analysis above, the optimal deformation conditions for globularization is 950–980 °C and 0.1–1 s^{-1}, under which near fully equiaxed microstructure with grain size around 1 μm can be achieved with a strain over 3. Meanwhile, the globularization kinetics is weakly dependent on deformation conditions within the optimum processing window. Decrease in globularized grain size with strain rate increasing was also found for Ti–6Al–4V alloy with a colony alpha structure in [5], but the globularized fraction was too low to form a macro refined structure due to limited compression deformation. Though the refined globularized microstructure has been reported obtained by deformation at warm temperature and low strain rate for colony structure [16] or at hot temperature and higher strain rate for martensite structure [17], this is the first time that the refined globularized microstructure is achieved under high temperature and higher strain rate conditions for colony structure at large strains (over 3). Because of thermal inertia in large billets, colony structures are most often produced even using water quenching after single beta processing. Thus the present finding should have more practical significance for cogging process of two phase titanium alloys in industry. As deformation time is very low at such higher strain rates, the interpretation of this near fully globularized microstructure is not enough by the reported mechanisms in [8–10] and [18] consisting of processes including intraphase boundaries formation and phase transformation which are time consuming. Thus, other globularization mechanisms for alloys deformed at higher strain rates deserve further study.

The SEM and TEM observation of the refined structure achieved via large strain deformation at 980 °C and 0.1 s^{-1} is shown in Fig. 7, and similar characteristic to research result in [17] for martensite structure can be found: discontinuously distributed beta phase due to dynamic recrystallization and high dislocation density at the globularized grain boundaries (indicated by the arrow in Fig. 7b). Thus according to the result in [17], this microstructure should also have improved superplasticity which is more favorable for the finally isothermal die forging.

4. Conclusion

Dynamic globularization kinetics of TC11 alloy has been studied in the temperature range of 920–980 °C and strain rate range of 0.01–10 s^{-1}. The following conclusions have bee drawn from the results of this investigation.

(1) The dynamic globularization kinetics TC11 alloy is sensitive to deformation conditions and follows an Avrami type sigmoid equation versus strain.
(2) Critical strains around 0.42–0.65 are needed for globularization initiation for all deformation conditions, and both globularization kinetics rate and globualrized grain size increase with increasing temperature and decreasing strain rate with sharp change at strain rate lower than 0.1 $s^{-1}$and temperature lower than 950 °C.
(3) Refined equiaxed structure can be achieved at the optimum processing parameters of 950–980 °C and 0.1–1 s^{-1} with a strain about or over 3, which is favorable for practical industry application.

References

[1] H.Z. Guo, Z.K. Yao, H. Su, Z. Su, J. Soc. Aeron. 18 (1997) 189.
[2] V.K. Berdin, M.V. Karavaeva, L.A. Syutina, Met. Sci. Heat Treat. 46 (2004) 54.
[3] I. Wesis, R. Srinivasan, P.J. Bania, D. Eylon, S.L. Semiatin (Eds.), Advances in the Science and Technology of Titanium Alloy Processing, The Minerals, Metals & Materials Society, 1997, p. p4.

[4] G. Lutjering, Mater. Sci. Eng. A243 (1998) 32.
[5] T. Seshacharyulu, S.C. Medeiros, W.G. Frazier, Y.V.R.K. Prasad, Mater. Sci. Eng. A325 (2002) 112.
[6] R. Wanjara, M. Jahazi, H. Monajati, S. Yue, Mater. Sci. Eng. A416 (2006) 300.
[7] C.H. Park, Y.G. Ko, C.S. Lee, K.T. Park, D.H. Shin, H.S. Lee, Mater. Sci. For. 551–552 (2007) 365.
[8] O.A. Kaybyshev, R.Y. Lutfullin, G.A. Salishchev, Fiz. Met. Metalloved. 59 (1985) 578.
[9] O.A. Kaybyshev, R.Y. Lutfullin, G.A. Salishchev, Fiz. Met. Metalloved. 66 (1988) 966.
[10] O.A. Kaybyshev, R.Y. Lutfullin, G.A. Salishchev, Fiz. Met. Metalloved. 66 (1988) 1163.
[11] S.L. Semiatin, J.F. Thomas, P. Dadras, Metall. Trans. 14A (1983) 2363.
[12] E.B. Shell, S.L. Semiatin, Metall. Mater. Trans. 30A (1999) 3219.
[13] S.L. Semiatin, V. Seetharaman, I. Weiss, Mater. Sci. Eng. A263 (1999) 257.
[14] N. Stefansson, S.L. Semiatin, D. Eylon, Metall. Mater. Trans. 33A (2002) 3527.
[15] S.L. Semiatin, N. Stefansson, R.D. Doherty, Metall. Mater. Trans. 36A (2005) 1372.
[16] G.A. Salishchev, S.Yu. Mironov, S.V. Zherebtsov, Rev. Adv. Mater. Sci. 11 (2006) 152.
[17] C.H. Park, Y.G. Ko, J.W. Park, C.S. Lee, Mater. Sci. Eng. A496 (2008) 150.
[18] I. Weiss, F.H. Froes, D. Eylon, G.E. Welsch, Metall. Trans. 17A (1986) 1935.
[19] J.H. Kim, S.L. Semiatin, C.S. Lee, Acta Mater. 51 (2003) 5613.